Colloids and Surfaces B: Biointerfaces 133 (2015) 12–18

Contents lists available at ScienceDirect

Colloids and Surfaces B: Biointerfaces

journal homepage: www.elsevier.com/locate/colsurfb

Stereoisomerism effect on sugar–lectin binding of self-assembled glyco-nanoparticles of linear and brush copolymers

Pengfei Sun, Mingchang Lin, Yu Zhao, Guosong Chen*, Ming Jiang

State Key Laboratory of Molecular Engineering of Polymers, Collaborative Innovation Center of Polymers and Polymer Composite Materials, Department of Macromolecular Science, Fudan University, Shanghai 200433, China

ARTICLE INFO

Article history:
Received 18 February 2015
Received in revised form 10 April 2015
Accepted 19 May 2015
Available online 27 May 2015

Keywords:
Glycopolymers
Glyco-nanoparticles
Stereoisomerism effect
Concanavalin A
FimH protein

ABSTRACT

Binding behavior of carbohydrate and protein is known to be crucial to the biological roles of sugars. Recently, we notice that, even to the same lectin, some reported binding results based on glycopolymers and/or self-assembled glyco-nanoparticles are different from those obtained on small molecular level. Some of such discrepancy could be associated with the different detection methods used. In this paper, by using self-assembled nanoparticles based on brush and linear glycopolymers, this stereoisomerism effect was evaluated systematically, both in solution and on solution-solid interface by different methods. All measurements led to the same conclusion that the stereoisomer of sugars determined the binding ability of glyco-nanoparticles with different lectins. The investigation also provided evidence on the different binding modes of nanoparticles of linear polymers and brush polymers.

© 2015 Elsevier B.V. All rights reserved.

1. Introduction

Glycans exist in nature mainly as macromolecules, which include polysaccharides, glycoproteins, glycolipids and proteoglycans [1–5]. They can be recognized by different lectins, which are crucial in many important biological processes. A significant portion of the biological functions of glycans is related to their binding to lectins. Generally such carbohydrate–lectin interactions share two features, i.e. specificity and multivalency. Specificity indicates that the interaction is greatly related to the configuration and conformation of sugars and the carbohydrate recognition domain (CRD) of lectins. Multivalency indicates the dramatically enhanced binding ability of the multiple sugars to different CRDs on the same protein [6–8]. Considering the fact that many of the currently known CRDs only bind to the terminal oligosaccharides of glycans, glycopolymers with repeating pendent units show their great advantage in mimicking these terminal oligosaccharides [9–12], which is important to further exploration on both of the known and unknown carbohydrate–protein interactions. Meanwhile, the artificial glycopolymers and glyco-nanoparticles have show enhancement multivalent binding behavior of carbohydrate and lectins [13–19].

However, by comparing the results based on glycopolymers and oligosaccharides, one could find some discrepancy in the specificity of carbohydrate–lectin interaction. For example, it was reported that glycopolymers with β-D-glucopyranoside [20–24] as pendent groups showed specific binding ability to Concanavalin A (Con A) either in their self-assembled or single chain state. However, Con A was previously believed to only have specific binding with α-D-mannopyranoside or α-D-glucopyranoside but not with their β-isomers of D-glucopyranoside [25]. For example, Barboiu had used quartz crystal microbalance (QCM) to conform that β-D-glucopyranoside modified gold nanoparticles or vesicles cannot bind with Con A [26,27].

Moreover, this inconsistency is not limited to plant lectins. FimH protein found on the surface of *Escherichia coli* (*E. coli*) has binding specificity to α-mannopyranoside [28] supported by protein crystallographic data of bound proteins. However, some previous reports based on glycopolymers containing β-D-glucopyranoside as pedant groups also showed strong binding tendency [29]. We noticed that these inconsistent data were based on different characterization methods. Indeed, the techniques to detect carbohydrate–protein interactions varies and can be generally divided into two categories, i.e. based on interactions in solution, which includes UV–vis spectroscopy etc.; and on the solid–liquid interface, i.e. surface plasmon resonance (SPR). Thus it is greatly demanding to design polymeric systems containing different stereoisomers of sugars to compare their binding ability to lectins by using different methods.

* Corresponding author. Tel.: +86 21 55664275.
E-mail address: guosong@fudan.edu.cn (G. Chen).

http://dx.doi.org/10.1016/j.colsurfb.2015.05.036
0927-7765/© 2015 Elsevier B.V. All rights reserved.

In this paper, self-assembled glyco-nanoparticles are prepared from brush or linear glyco-block copolymers with stereoisomers of sugars attached as repeating pedant groups. The repeating sugar moieties provide enough multivalent effect and ensure the interactions detectable. Different architectures of natural glycans are known in literature, which include linear and branched polysaccharides, and polymer brush, i.e. proteoglycans. However, binding ability of their artificial mimic to lectins, i.e. self-assembled glycopolymers with different architectures has not been extensively explored so far. Since the carbohydrate–protein interaction can be significantly enhanced by the multivalent effect, different architectures may have different impact on the multivalent enhancement, which also deserve exploration. In addition, comparison of binding results from different polymeric architectures may confirm the binding behavior of different glyco-stereoisomers.

2. Results and discussion

In our previous research, triblock copolymer having conjugated polyfluorene central block and glycopolymers as side blocks was proved to be a nice platform to investigate the binding ability of glyco-regioisomers to lectins [30], because the copolymers enjoy its readiness in assembly into nanoparticles in water with fluorescent emission which benefits the subsequent studies. For the purpose of studying the architectural effect, corresponding brush copolymer with a conjugated main chain and glycopolymer grafts were prepared. The structures of both linear triblock copolymer i.e. polyfluorene-*b*-glycopolymers with polyfluorene (PF) as the middle block and glycopolymer as side blocks, and brush copolymer with polybenzene-*co*-*alt*-fluorene (PPF) backbone carrying glycopolymer grafts are shown in Scheme 1.

The structures of four sugar isomers (α-glucopyranoside, β-glucopyranoside, α-mannopyranoside and α-galactopyranoside) linked to the main chain of brush glycopolymers **B-α-Glc**, **B-β-Glc**, **B-α-Man**, **B-α-Gal** are shown in Scheme 1. Their corresponding linear block glycocopolymers are denoted as **L-α-Glc**, **L-β-Glc**, **L-α-Man**, **L-α-Gal**. The synthetic route by a combination of atom transfer radical polymerization (ATRP) and click reaction toward brush and linear copolymers is shown in Schemes S1 and S2. The PPF macroinitiator precursor (PPF-OH) was first prepared by Suzuki coupling reaction followed by esterification (Scheme S3, ^{1}H NMR in Fig. S1) with M_n and PDI determined as 11 600 and 1.6, respectively by GPC (Fig. S2). After esterification of PPF-OH, the peaks in the ^{1}H NMR spectrum of the obtained macroinitiator (GPC in Fig. S3) assigned to the alkoxyl protons (phenyl—O—C***H***$_2$—C***H***$_2$—C***H***$_2$OH) all shifted to downfield, indicating the successful synthesis of PPF-macroinitiator (Fig. S4). Then brush copolymer PPF-PGMA (PGMA: poly(glycidyl methacrylate)) was prepared by ATRP. M_n and PDI of PPF-PGMA brush copolymer were 34 800 and 1.9 respectively, determined by GPC (Fig. S5). In the ^{1}H NMR spectrum of PPF-PGMA (Fig. S6), the peaks of PGMA at δ 4.30, 3.81 (—OCO—C***H***$_2$—), 3.23 (—C***H***—CH$_2$—O—), 2.84, 2.63 (—CH—C***H***$_2$—O—) appeared obviously, which indicated the successful synthesis of PGMA chain. DP of each PGMA chain was estimated to be 6 by comparing the integration area of —CH—C***H***$_2$—O— to that of phenyl—O—C***H***$_2$—. Thus the weight ratio of PGMA chain was calculated as 80%. Then, by opening the

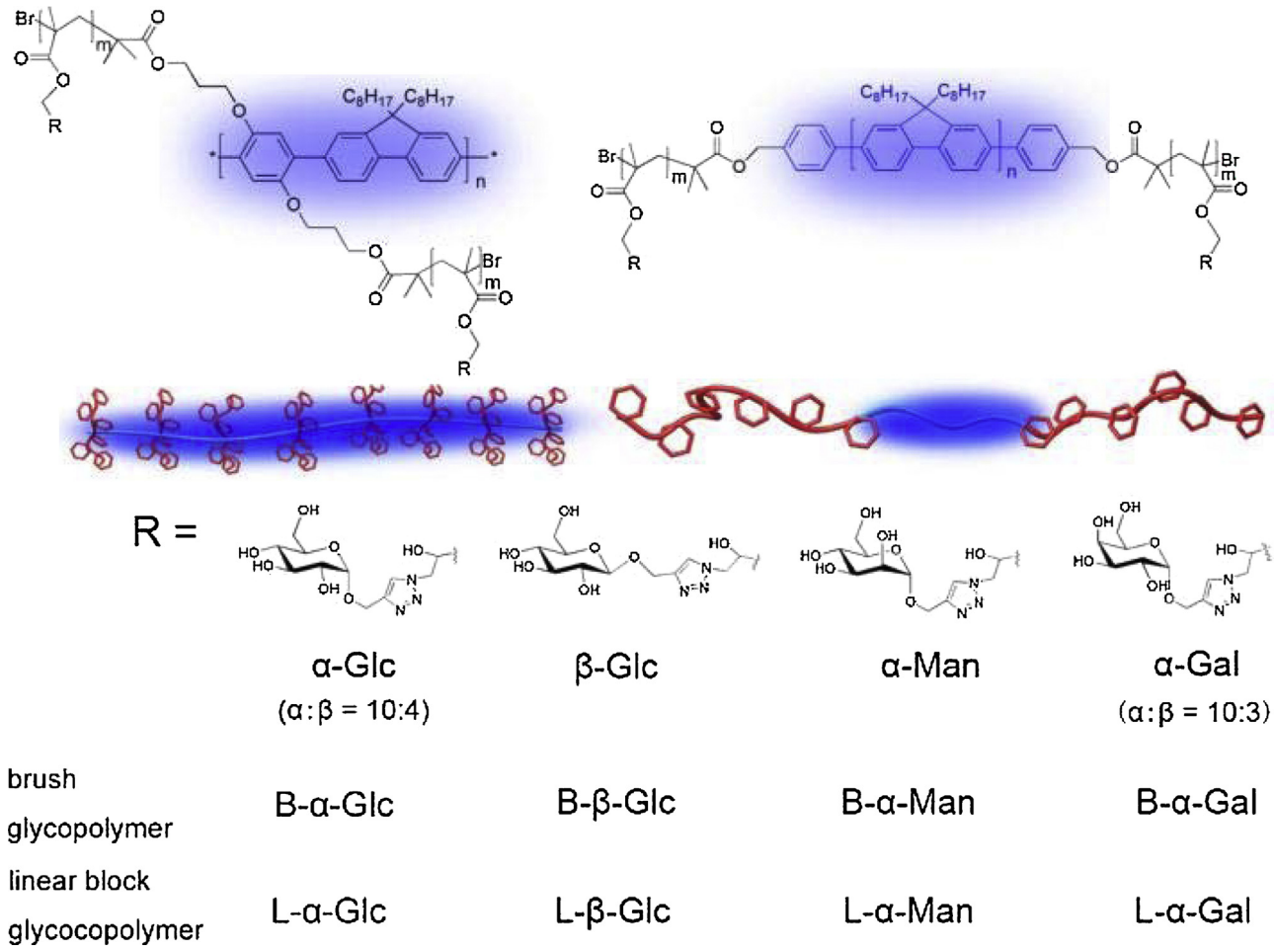

Scheme 1. Chemical structures of PPF-brush glycopolymers (**B-α-Glc**, **B-β-Glc**, **B-α-Man**, **B-α-Gal**) and PF-triblock glycopolymers (**L-α-Glc**, **L-β-Glc**, **L-α-Man**, **L-α-Gal**).

epoxide rings on PGMA using sodium azide, brush copolymer PPF-PGMA-N_3 was obtained (Fig. S7). Four kinds of alkyne-modified sugars (^{1}H NMR in Fig. S8) were separately grafted to PPF-PGMA-N_3 by click reaction to give the corresponding PPF-brush glycopolymers **B-α-Glc**, **B-β-Glc**, **B-α-Man**, and **B-α-Gal** (^{1}H NMR in Fig. S9). Moreover, the linear PF-sugar copolymers **L-α-Glc**, **L-β-Glc**, **L-α-Man**, **L-α-Gal** were synthesized following our reported procedures [30], i.e. started from PF macroinitiator (PF-OH), followed by polymerization of PGMA blocks. Glyco-modification to the side block was the same as that of brush copolymer, i.e. polymerization of GMA, followed by epoxide ring-opening and click reaction. It is worth to mention that the DP of the PGMA block was about 40, with the weight ratio of PGMA in PF copolymer was 82%. Thus, the brush family and block family shared a similar glyco-content.

With the block and brush glycopolymers in hand, their self-assembly in water was further performed. Typically, amphiphilic **B-α-Glc** was dissolved in DMF (1 mg/mL), and then dialyzed against HBS buffer for 2 d. A certain amount of HBS buffer was added into the solution to adjust the final concentration to 0.5 mg/mL. Aggregates of **B-α-Glc** formed under this condition. The hydrodynamic radius ($\langle R_h \rangle$) of the aggregates in solution was measured by DLS as 27 nm with PDI around 0.24 (Fig. S10). The TEM image showed well-dispersed spheres (Fig. S11). These results indicated that **B-α-Glc** self-assembled into nanoparticles stabilized by the surface-riched hydrophilic glyco-brushes, which was denoted as **B-NP-α-Glc**.

Table 1
DLS and TEM characterization of nanoparticles formed by brush and linear glycopolymer.

Nanoparticles	α-Glc	β-Glc	α-Man	α-Gal
B-NP				
$\langle R_h \rangle$ (nm)	27	42	37	30
PD.I.$_{DLS}$	0.24	0.25	0.20	0.20
D_{TEM} (nm)	24	29	25	24
L-NP				
$\langle R_h \rangle$ (nm)	28	41	38	25
PD.I.$_{DLS}$	0.25	0.30	0.30	0.23
D_{TEM} (nm)	30	29	29	25

Similarly, nanoparticles **B-NP-β-Glc** ($\langle R_h \rangle$ = 42 nm), **B-NP-α-Man** ($\langle R_h \rangle$ = 37 nm) and **B-NP-α-Gal** ($\langle R_h \rangle$ = 30 nm) formed via the self-assembly of the corresponding glycopolymers respectively (Table 1, Figs. S10 and S11). Meanwhile, nanoparticles also formed by linear copolymers (L-NPs) with $\langle R_h \rangle$ ranging from 25 nm to 41 nm, which were denoted as **L-NP-α-Glc, L-NP-β-Glc, L-NP-α-Man** and **L-NP-α-Gal** (Table 1, Figs. S12 and S13). The particles were quite stable as their size kept constant within four months monitored by DLS. TEM observations revealed that the dispersed nanostructures of the assemblies for both B-NPs and L-NPs exhibited smaller sizes than those from DLS (Figs. S10–S13). This inconsistence is reasonable, as the nanoparticles in solution are solvated but not

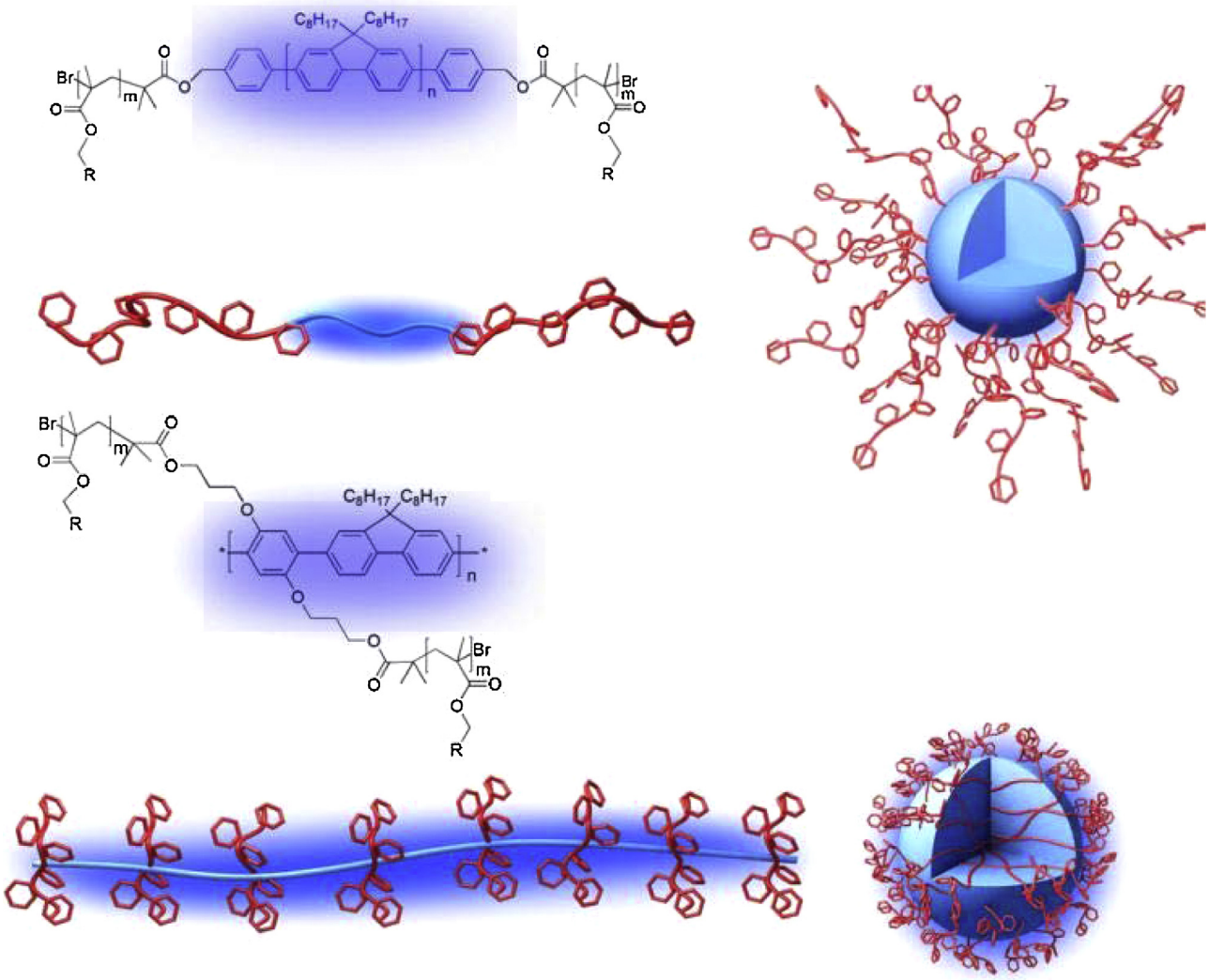

Scheme 2. Cartoon representation of L-NP (top) and B-NP (bottom).

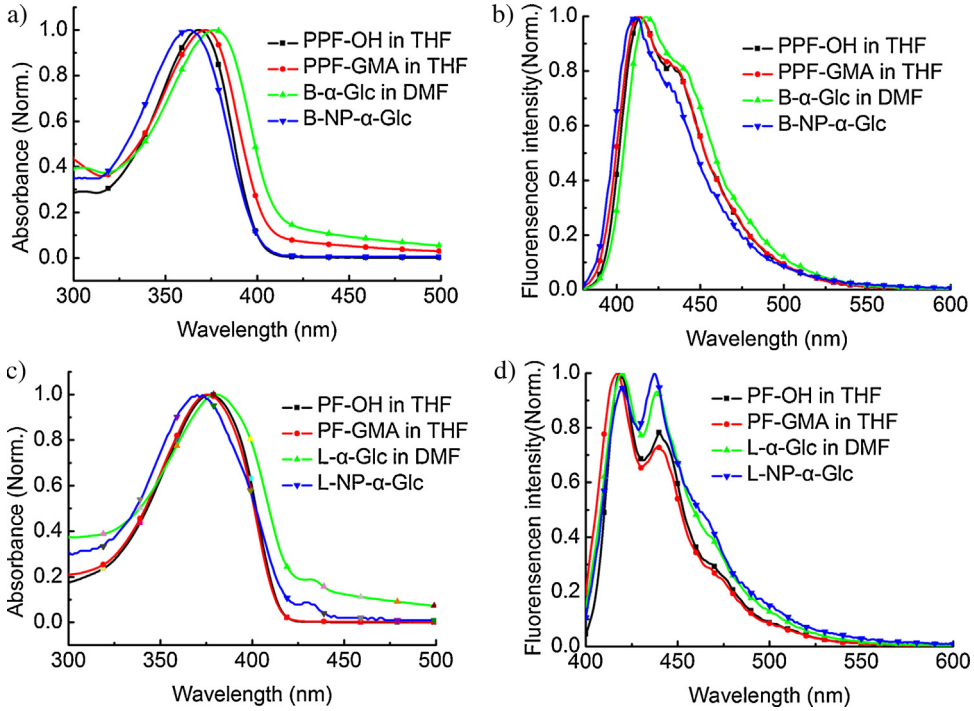

Fig. 1. Normalized (a) UV–vis absorption and (b) photoluminescence spectra of PPF-OH (0.05 mg/mL in THF), PPF-PGMA (0.05 mg/mL in THF), **B-α-Glc** copolymer solution (0.05 mg/mL in DMF) and **B-NP-α-Glc** (0.05 mg/mL in HBS buffer). The fluorescence emissions were excited at 360 nm. Normalized (c) UV–vis absorption and (d) photoluminescence spectra of PF-OH (0.05 mg/mL in THF), PF-PGMA (0.05 mg/mL in THF), **L-α-Glc** copolymer solution (0.05 mg/mL in DMF) and **L-NP-α-Glc** (0.05 mg/mL in HBS buffer). The fluorescence emissions were excited at 375 nm.

in dried state. Therefore, these stable nanoparticles from the linear and brush copolymers sharing a similar sugar content and particle size become ideal candidates for evaluating the effects of sugar isomers as well as polymer chain architectures (brush/linear) on the carbohydrate–protein interactions in self-assembled state. Scheme 2 shows the schematic model of L-NPs and B-NPs. We would like to note the possible difference between L-NPs and B-NPs. Glyco-chain in the linear copolymer (DP = 40) is much longer than that of the brush copolymer (DP = 6) and each linear copolymer has two long glyco-chains only, while each PPF unit of the brush copolymer has several short sugar chains. Therefore, clear core–shell structure for B-NP was not expected and the nanoparticle was stabilized by a thin and dense layer of glyco-brush. Meanwhile, L-NP may have clear core–shell structure with loose and sparse hydrophilic glyco-block forming the shell (Scheme 2). This basic difference may lead to different binding behavior to lectins.

The UV–vis absorption and photoluminescence (PL) emission spectra of PPF-OH in THF, PPF-PGMA in THF, **B-α-Glc** in DMF and **B-NP-α-Glc** in water are shown in Fig. 1a and b. The absorption peak of PPF-OH in THF was around 368 nm and the corresponding photoluminescence peak was around 414 nm. PPF-PGMA retained the similar absorption and emission spectra to those of PPF. For **B-α-Glc** in DMF, its absorption peak appeared at 372 nm, while its emission peak showed at 418 nm as well. After the self-assembled **B-NP-α-Glc** formed in water, the absorption and PL peaks blue shifted to 360 nm and 410 nm, respectively. This phenomenon may be explained as quite strong aggregation of the PPF chains of **B-NP-α-Glc** due to enhanced π–π interactions and/or hydrophobic interactions of the PPF segments. Similarly, as shown in Fig. 1c and d, after **L-α-Glc** assembled into nanoparticle **L-NP-α-Glc**, an obvious blue shift was also observed between their corresponding absorption peaks, i.e. from 380 nm (in DMF) to 370 nm (in water). Meanwhile the main PL spectra peaks shifted from 440 nm (in DMF) to 420 nm (in water). This hypsochromic shift after self-assembly could be explained by the H-type aggregation formed by a parallel orientation of PF segments [31,32].

The binding abilities of the nanoparticles containing α-Glc and β-Glc formed by L-NPs and B-NPs are compared by using Concanavalin A (Con A) as a model lectin. In the study, different detection methods, including fluorescence, DLS, UV–vis, SPR are employed. According to the early results from glycobiology studies with various isothermal titration calorimetry (ITC) and crystallography data between Con A and different mono- or oligosaccharides, α-Man binds to Con A stronger than α-Glc, while β-Glc and α-Gal do not bind [33–35]. However, when these sugars have been attached to polymer chains, their binding behavior to Con A could be different. For example, linear block copolymer containing poly(*N*-isopropylacrylamide) block and β-D-glucopyranoside-modified glyco-block [29], star polymers and micelles with β-D-glucopyranoside-modified repeating units [21–23] were reported to bind with Con A which was led by the turbidity test by UV–vis spectra in solution or QCM on surface.

We report our fluorescence results first. As shown in Fig. S14, no obvious intensity decrease of all of the B-NPs and L-NPs was observed after Con A addition, which is very different from the previous reports on the interactions between lectins and soluble sugar-containing linear conjugated polymers [36–38]. This phenomenon, which was observed in our previous paper as well, is understandable because in the current case, the fluorescent emitting conjugated species aggregated in the core of the nanoparticles, so Con A, which may interact with the sugar units on the nanoparticle surfaces would not influence the aggregation state of the conjugated polymers [12].

In our previous research, DLS was proved effective to measure carbohydrate–protein interactions on the surface of nanoparticles [30,39]. As shown in Fig. 2, after addition of Con A, the scattered light intensity (I_s/I_0) and hydrodynamic radius ($\langle R_h \rangle$) of **B-NP-α-Glc** and **B-NP-α-Man** were increased, while those of **B-NP-β-Glc** and **B-NP-α-Gal** did not change. The increase trend of **B-NP-α-Glc** and

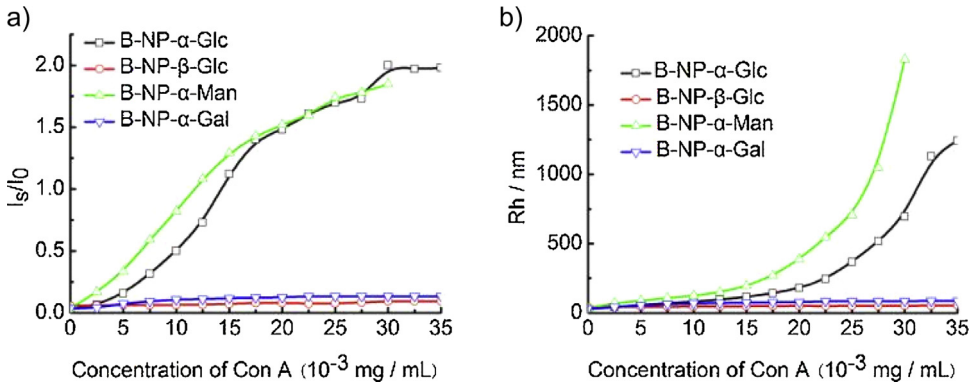

Fig. 2. Evolution of (a) relative scattered intensity (I_s/I_0) and (b) $\langle R_h \rangle$ of B-NPs (0.05 mg/mL) after addition of Con A in HBS buffer.

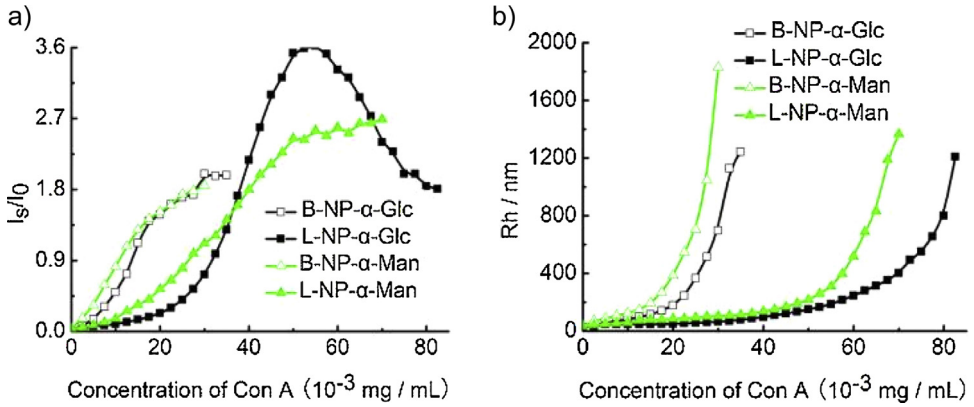

Fig. 3. Evolution of (a) relative scattered light intensity (I_s/I_0) and (b) $\langle R_h \rangle$ of **B-/L-NP-α-Glc** and **B-/L-NP-α-Man** (0.05 mg/mL) after addition of Con A in HBS buffer.

B-NP-α-Man were similar to each other, indicating a quite similar binding behavior of the two types of nanoparticles. Similar phenomenon was also observed when Con A was added to the solution of L-NPs (Fig. S15). These results clearly showed that **B/L-NP-α-Glc** and **B/L-NP-α-Man** bind to Con A strongly, while **B/L-NP-β-Glc** and **B/L-NP-α-Gal** do not.

Fig. 3 compares the binding ability to Con A between B-NPs and L-NPs. When Con A was titrated to the solution of L-/B-NPs, the evolution of I_s/I_0 and $\langle R_h \rangle$ of **B-NP-α-Man/Glc** was obviously faster than those of **L-NP-α-Man/Glc**. In other words, at a given concentration, Con A addition caused more obvious particle aggregation for **B-NP-α-Man/Glc** than **L-NP-α-Man/Glc**. This different binding behavior, in our opinion, could be attributed to the structural dissimilarity between B-NP and L-NP. When Con A was first titrated to the solution of L-NPs, Con A could be probably trapped in the lose shell of the glycopolymer blocks, which of course has little contribution to the nanoparticle aggregation. However, for B-NPs the inter-nanoparticle binding could be dominant as there is only a dense and thin glyco-riched layer on the surface of B-NPs (Scheme 3). It is worth to mention that the obvious decrease of I_s/I_0 could be attributed to the precipitation of nanoparticles after binding to Con A. However, at the same time, the $\langle R_h \rangle$ was still increasing showing the prevalent size increase of nanoparticles in the solution.

As shown in Fig. 4, when Con A was added to the solution of L-NPs or B-NPs, an apparent decrease of transmittance was observed for the samples of **B-NP-α-Man/Glc**. However, **B-NP-β-Glc** and **B-NP-α-Gal** did not exhibit any decrease of transmittance under this condition. Moreover, similar result was observed from L-NPs (Fig. 4b). This phenomenon was quite consistent to those from DLS. Furthermore, at rather low concentration ([Con A] < 40 μg/mL), the decrease rate of transmittance in the solution of B-NPs, i.e. B-NP-α-Man/Glc was faster than that of L-NPs, i.e. **L-NP-α-Man/Glc**. When the Con A concentration reached the range of 40–60 μg/mL, the transmittance of B-NPs exhibited saturation at around 60%, while that of L-NPs kept decreasing when more Con A was added. This result also supports the possible nanoparticle–lectin interaction mode we proposed in Scheme 3.

In this work we devote to compare the binding results from solution to those from the liquid–solid interface. SPR is employed as two representative methods on the liquid–solid interface. In each method, Con A was first immobilized on 11-mercaptoundecanoic acid (MUA) modified gold chip via nucleophilic substitution present on Con A surface [40]. As shown in Fig. 5 for SPR, **B-NP-α-Man/Glc** exhibited obvious response increase, i.e. mass absorption while **B-NP-β-Glc** did not. Similar phenomenon was again observed by the results from L-NPs. This result was consistent to the results from DLS and turbidity test. Moreover, larger mass absorption of

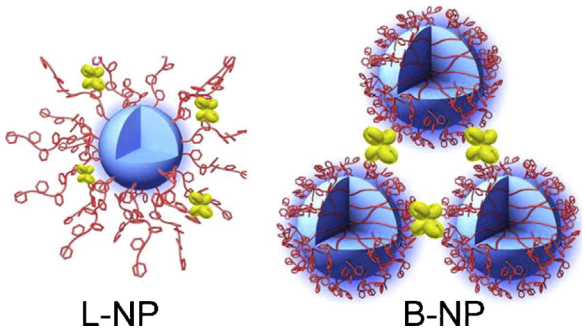

Scheme 3. Two different nanoparticle-lectin Con A interacting modes of L-NPs and B-NPs. Turbidity test supported the proposed binding modes.

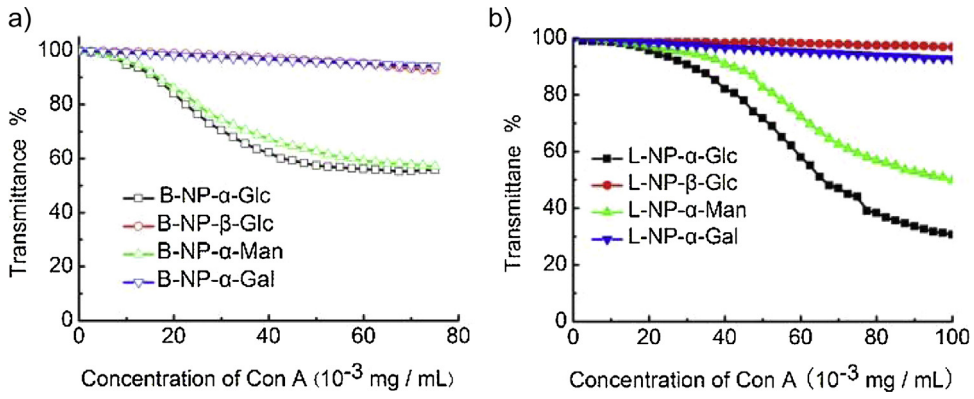

Fig. 4. UV turbidity test of (a) B-NPs and (b) L-NPs at 0.05 mg/mL in HBS buffer after addition of Con A.

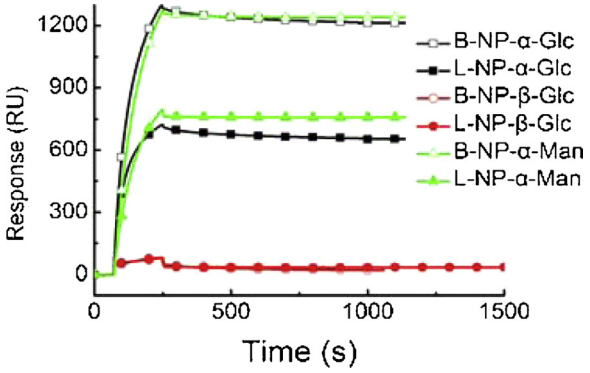

Fig. 5. SPR study of B-/L-NPs (0.05 mg/mL) in HBS buffer flowing with Con A.

B-NP-α-Man/Glc than **L-NP-α-Man/Glc** on surface was also observed (Fig. 5).

Having successfully examined the binding ability of nanoparticles with Con A in water, we tried to investigate their binding and labeling properties to cell-surface lectins of bacteria (FimH). Two *E. coli* strains ORN 178 and ORN 208 are chosen as a model system. The ORN 178 strain expresses FimH protein, which has binding specificity to α-mannopyranoside, while the ORN 208 strain does not [28]. Previous investigation proves that the mannopyranose ring makes several direct hydrogen bonds to the side chains of amino acid residues in the binding site of FimH and additional indirect water-mediated hydrogen bonds. All of the hydroxyl groups of the mannopyranose ring, rather than the anomeric position, interact extensively with the carbohydrate recognition domain (CRD) of FimH [41]. However, other previous reports mentioned that linear block copolymers containing β-glucopyranoside pedant groups and their self-assembled nanoparticles bound to FimH [20,29]. Due to the excitation wavelength of Confocal Microscope was not suitable for PPF of B-NPs, only L-NPs were employed in this study. As shown in Fig. 6a and c, **L-NP-α-Man** and **L-NP-α-Glc** successfully bound to *E. coli* ORN 178 and labeled the bacteria with blue fluorescence. On the contrary, both of them did not bind to ORN 208 strain, showing the specificity of this binding (Fig. 6b, d). From our results, it is clear that **L-NP-α-Glc** bound almost as successful as **L-NP-α-Man**, apparently change of one hydroxyl group has been tolerated under the help of multivalency. However, **L-NP-β-Glc** did not show any specific binding to

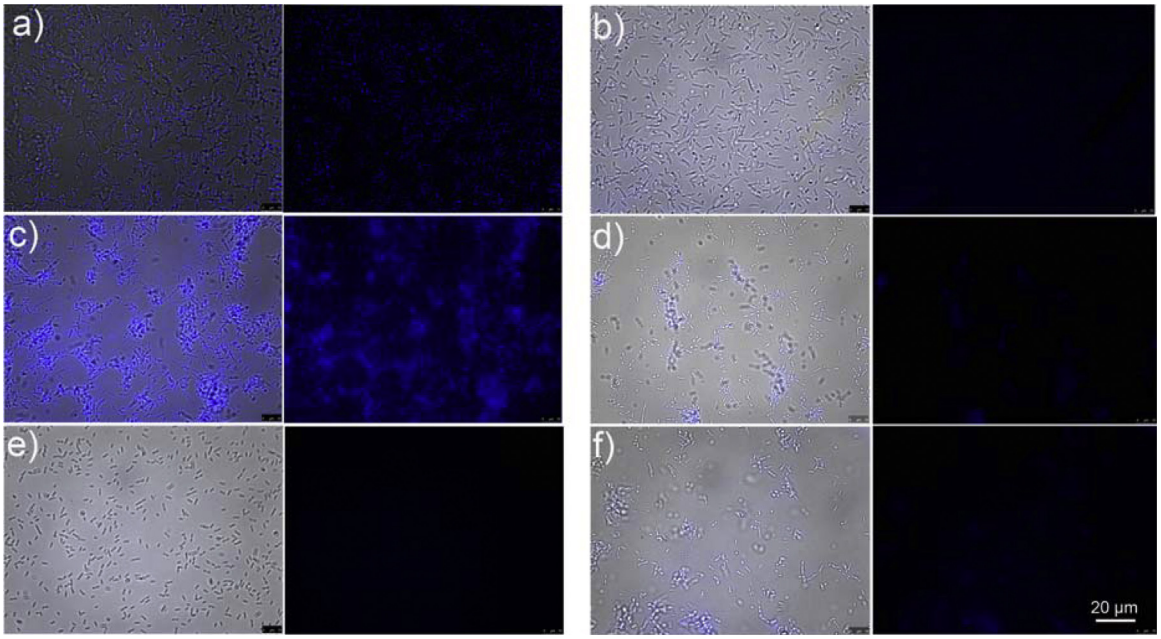

Fig. 6. Confocal fluorescence microscopy images of **L-NP-α-Glc** incubated with (a) ORN 178 and (b) ORN 208, **L-NP-α-Man** with (c) ORN 178 and (d) ORN208, (e) **L-NP-β-Glc** and (f) **L-NP-α-Gal** with ORN 178. For every sample, the bright field and dark field are presented at the same time (scale bar: 20 μm).

the ORN 178 strain, similar to L-**NP-α-Gal** (Fig. 6e, f), which means that the configuration of anomeric center seems to be crucial to the binding ability of sugars to FimH protein. We may propose that, in this case selectivity weights heavier than multivalency. Moreover the result based on FimH is consistent to our previous result on Con A, verifying the importance of stereoisomers on the binding effect of sugars of self-assemblies.

3. Conclusions

As a conclusion, by using self-assembled glyco-nanoparticles based on brush and linear copolymers, glyco-stereoisomerism effect on lectin binding was evaluated by a combination of methods. It is clear that to nanoparticles containing α-/β-glucopyranoside as pendant groups, the anomeric center plays a crucial role to their binding ability, not only to model lectin Con A, but also the FimH lectin on bacteria. Although multiple sugars as side groups enhance their binding ability via multivalent effect, the selectivity of carbohydrate–protein interaction seems to play a major role. This conclusion was proved via characterization methods of DLS and turbidity test in solution, and SPR on solid-solution interface as well.

Acknowledgements

Ministry of Science and Technology of China (2011CB932503), National Natural Science Foundation of China (Nos. 91227203, 51322306), Innovation Program of Shanghai Municipal Education Commission and the Shanghai Rising-Star Program (Grant 13QA1400600) are acknowledged for their financial supports.

Appendix A. Supplementary data

Supplementary data associated with this article can be found, in the online version, at http://dx.doi.org/10.1016/j.colsurfb.2015.05.036

References

[1] N.C. Reichardt, M.M. Lomas, S. Penadés, Chem. Soc. Rev. 429 (2013) 4358.
[2] R.A. Dwek, Chem. Rev. 96 (1996) 683.
[3] W.S. Lu, X.L. Zhang, Prog. Chem. 17 (2005) 1054.
[4] S. Jeon, C.Y. Yoo, S.N. Park, Colloids Surf. B: Biointerfaces 129 (2015) 7.
[5] L. Bekale, D. Agudelo, H.A. Tajmir-Riahi, Colloids Surf. B: Biointerfaces 125 (2015) 309.
[6] L.L. Kiessling, J.C. Grim, Chem. Soc. Rev. 42 (2013) 4476.
[7] M. Marradi, F. Chiodo, I. García, S. Penadés, Chem. Soc. Rev. 42 (2013) 4728.
[8] X.R. Zhang, X.Y. Li, S.D. Zhu, C.X. Li, H.S. Guan, Chin. J. Org. Chem. 2 (2004) 119.
[9] S.R. Simon Ting, G.J. Chen, M.H. Stenzel, Polym. Chem. 1 (2010) 1392.
[10] S.I. Spain, M.I. Gibson, N. Cameron, J. Polym. Sci. A: Polym. Chem. 45 (2007) 2057.
[11] V. Ladmiral, E. Melia, D.M. Haddleton, Eur. Polym. J. 40 (2004) 431.
[12] F. Lei, D.F. Pei, T.F. Shi, Z. Guo, Chem. J. Chin. Univ. 32 (2011) 1667.
[13] Y.Y. Wang, Q.L. Fan, P. Wang, L.H. Wang, W. Huang, Chem. J. Chin. Univ. 28 (2007) 1377.
[14] J.J. Lundquist, E.J. Toone, Chem. Rev. 102 (2002) 555.
[15] O. León, A.M. Bonilla, V. Bordegé, M.F. García, J. Polym. Sci. A: Polym. Chem. 49 (2011) 2627.
[16] X. Wang, O. Ramström, M.D. Yan, J. Mater. Chem. 19 (2009) 8944.
[17] R.V. Vico, J. Voskuhl, B.J. Ravoo, Langmuir 27 (2011) 1391.
[18] D.F. Pei, Y.C. Li, Q.R. Huang, Q. Ren, F. Li, T.F. Shi, Colloids Surf. B: Biointerfaces 127 (2015) 130.
[19] D.F. Pei, Y.C. Li, Q.R. Huang, Q. Ren, F. Li, T.F. Shi, Colloids Surf. B: Biointerfaces 126 (2015) 367.
[20] G. Pasparakis, A. Cockayne, C. Alexander, J. Am. Chem. Soc. 129 (2007) 11014.
[21] Y. Chen, G.J. Chen, M.H. Stenzel, Macromolecules 43 (2010) 8109.
[22] Y. Fang, W. Xu, X.L. Meng, X.Y. Ye, J. Wu, Z.K. Xu, Langmuir 28 (2012) 13318.
[23] J. Kumar, A. Bousquet, M.H. Stenzel, Macromol. Rapid Commun. 32 (2011) 1620.
[24] B.B. Ke, L.X. Wan, W.X. Zhang, Z.K. Xu, Polymer 51 (2010) 2168.
[25] T.K. Dam, C.F. Brewer, Chem. Rev. 102 (2002) 387.
[26] E. Mahon, T. Aastrup, M. Barboiu, Chem. Commun. 46 (2010) 5491.
[27] E. Mahon, T. Aastrup, M. Barboiu, Chem. Commun. 46 (2010) 2441.
[28] C.S. Hung, J. Bouckaert, D. Hung, J. Pinkner, C. Widberg, A. Defusco, C.G. Auguste, R. Strouse, S. Langermann, G. Waksman, S.J. Hultgren, Mol. Microbiol. 44 (2002) 903.
[29] G. Pasparakis, C. Alexander, Angew. Chem. Int. Ed. 47 (2008) 4847.
[30] P.F. Sun, Y. He, M.C. Lin, Y. Zhao, Y. Ding, G.S. Chen, M. Jiang, ACS Macro Lett. 3 (2014) 96.
[31] Y.Q. Tian, C.Y. Chen, H.L. Yip, W.C. Wu, W.C. Chen, A.K.J. Jen, Macromolecules 43 (2010) 282.
[32] Y.C. Tung, W.C. Wu, W.C. Chen, Macromol. Rapid Commun. 27 (2006) 1838.
[33] H. Lis, N. Sharon, Chem. Rev. 98 (1998) 637.
[34] G. Chen, N.L. Pohl, Org. Lett. 10 (2008) 785.
[35] D.A. Mann, M. Kanai, D.J. Maly, L.L. Kiessling, J. Am. Chem. Soc. 120 (1998) 10575.
[36] R.L. Phillips, I.B. Kim, B.E. Carson, B. Tidbeck, Y. Bai, T.L. Lowary, L.M. Tolbert, U.H.F. Bunz, Macromolecules 41 (2008) 7316.
[37] C.H. Xue, F.T. Luo, H.Y. Liu, Macromolecules 40 (2007) 6863.
[38] C.H. Xue, S.P. Jog, P. Murthy, H.Y. Liu, Biomacromolecules 7 (2006) 2470.
[39] L. Su, Y. Zhao, G.S. Chen, M. Jiang, Polym. Chem. 3 (2012) 1560.
[40] Y.Z. Gou, S. Slavin, J. Geng, L. Voorhaar, D.M. Haddleton, C.R. Becer, ACS Macro Lett. 1 (2012) 180.
[41] O. Renaudet, N. Spinelli, Synthesis and Biological Applications of Glycoconjugates, Bentham Science, 2011, chapter 2.